Eur. Phys. J. A (2016) **52**: 242
DOI 10.1140/epja/i2016-16242-7

THE EUROPEAN PHYSICAL JOURNAL A

Review

Relativistic ion collisions as the source of hypernuclei*

A.S. Botvina[1,2,a], M. Bleicher[1], J. Pochodzalla[3,4], and J. Steinheimer[1]

[1] Frankfurt Institute for Advanced Studies, J.W. Goethe University, D-60438 Frankfurt am Main, Germany
[2] Institute for Nuclear Research, Russian Academy of Sciences, 117312 Moscow, Russia
[3] Helmholtz-Institut Mainz, J. Gutenberg-Universität, 55099 Mainz, Germany
[4] Institut für Kernphysik and PRISMA Cluster of Excellence, J. Gutenberg-Universität Mainz, D-55099 Mainz, Germany

Received: 1 October 2015 / Revised: 4 November 2015
Published online: 22 August 2016 – © Società Italiana di Fisica / Springer-Verlag 2016
Communicated by D. Blaschke

Abstract. We shortly review the theory of hypernuclei production in relativistic ion collisions, that is adequate to future experiments at BM@N, NICA, and FAIR. Within a hybrid approach we use transport, coalescence and statistical models to describe the whole process. We demonstrate that the origin of hypernuclei can be explained by typical baryon interactions, that is similar to the production of conventional nuclei. In particular, heavy hypernuclei are coming mostly from projectile and target residues, whereas light hypernuclei can be produced at all rapidities. The yields of hypernuclei increase considerably above the energy threshold for Λ hyperon production, and there is a tendency to saturation of yields of hypernuclei with increasing the beam energy up to few TeV. There are unique opportunities in relativistic ion collisions which are difficult to realize in traditional hypernuclear experiments: The produced hypernuclei have a broad distribution in masses and isospin. They can even reach beyond the neutron and proton driplines and that opens a chance to investigate properties of exotic hypernuclei. One finds also the abundant production of multi-strange nuclei, of bound and unbound hypernuclear states with new decay modes. In addition, we can directly get an information on the hypermatter both at high and low temperatures.

1 Introduction

The scope of contemporary nuclear physics extends from fundamental particles quarks and gluons to the most spectacular cosmic events, like supernova explosions. Remnants of these cosmic catastrophes are neutron stars. Having a core with supra-nuclear densities and a crust with sub-nuclear densities, these stellar objects merge all aspects of nuclear physics. The recent observations of two-solar-mass neutron stars [1, 2] significantly constrain the stiffness of the equation of state of hadronic matter at high densities. But even these remarkable observations do not allow a conclusive statement on the flavor composition of neutron stars. This still limited knowledge reflects our incomplete understanding of the underlying baryon-baryon and even more subtle multi-body interactions in baryonic systems, not to mention their relation to the elementary quark-gluon dynamics, *i.e.*, the flavor mixing. Detailed studies of the three-flavor nuclear equation of state will be mandatory to approach the structure of neutron stars, as well as to develop fundamental QCD theories. Essential modifications for the nuclear Equation of State (EoS) at high density and low temperature may be expected from the properties of three-baryon interactions [3–7]. Baryons with strangeness embedded in the nuclear environment, *i.e.*, hypernuclei, are the only available tool to approach the many-body aspect of the three-flavor strong interaction. Hypernuclei are formed when hyperons ($Y = \Lambda, \Sigma, \Xi, \Omega$) produced in high-energy interactions are captured by nuclei. They live significantly longer than the typical reaction times, therefore, they can serve as a tool to study the hyperon-nucleon and hyperon-hyperon interactions at low energies.

The investigation of hypernuclei is one of the rapidly progressing fields of nuclear physics, since they provide complementary methods to improve traditional nuclear studies and open new horizons for studying particle physics and nuclear astrophysics (see, *e.g.*, [8–16] and references therein). Precision experimental studies of hypernuclei confronted with precision structure calculations based on basic principles of QCD will, at the same time, help to explore the dominant two-baryon interaction in nuclei and disentangle, *e.g.*, three-baryon forces and charge symmetry breaking effects. Another pillar of contemporary hypernuclear studies is the exploration of the limits of stability in isospin and strangeness space.

* Contribution to the Topical Issue "Exploring strongly interacting matter at high densities - NICA White Paper" edited by David Blaschke *et al.*

[a] e-mail: a.botvina@gsi.de

Presently, hypernuclear physics is still focused on spectroscopic information and is dominated by a quite limited set of reactions [8, 11]. These are reactions induced by high-energy hadrons and leptons leading to the production of few particles, including kaons which are often used for tagging the production of hypernuclei in their ground and low excited states. In this case hypersystems with baryon density around the nuclear saturation density, $\rho_0 \approx 0.15\,\mathrm{fm}^{-3}$ are formed. Therefore, most previous theoretical studies concentrated on the calculation of the structure of nearly cold hypernuclei. Recently they started to develop new experimental methods: Heavy fissioning hypernuclei were identified with a relatively high probability in reactions induced by stopped antiprotons and by protons with energy around the threshold [17, 18]. Very encouraging results on hypernuclei come from experiments with light relativistic projectiles: In addition to well-known hypernuclei [19, 20], evidence for unexpected exotic hypernuclear states, like a Λ hyperon with two neutrons, was reported [21], which was never observed in other reactions. The production of such new exotic states (see also [22]) could be naturally explained within the breakup of excited hypernuclear systems [21, 23]. The case of double hypernuclei illustrates the complementarity of the various methods: Experiments using kaon beams and nuclear emulsions provide information on the ground-state masses of double hypernuclei [24]. The spectrum of excited states will be explored by the PANDA experiment at FAIR using antiprotons and performing high-resolution γ-spectroscopy [25]. Two-particle correlation studies between single hypernuclei and Λ-hyperons may —like conventional two-particle correlation studies in heavy-ion reactions (see, *e.g.*, [26])— provide unique information on particle-unstable resonances in double hypernuclei.

Many experimental collaborations (*e.g.*, STAR at RHIC [27]; ALICE at LHC [28]; PANDA [29], FOPI/CBM, and Super-FRS/NUSTAR at FAIR [30,31]; BM@N and MPD at NICA [32]) have started or plan to investigate hypernuclei and their properties in reactions induced by relativistic hadrons and ions. The limits in isospin space, particle unstable states, multiple strange nuclei and precision lifetime measurements are unique topics of these fragmentation reactions. All these experiments tell us that the production of hypernuclei in relativistic collisions is confirmed, and that this mechanism is very promising for exploring novel hypernuclear states.

It is important in this respect to note that the very first experimental observation of a hypernucleus was obtained in the 1950s in reactions of nuclear multifragmentation induced by cosmic rays [33]. Recently remarkable progress was made in the investigation of the multifragmentation reactions associated with relativistic heavy-ion collisions (see, *e.g.*, [34–37] and references therein). This gives us an opportunity to apply well-known theoretical methods adopted for description of these reactions also for production of hypernuclei [38–40]. Specially, we emphasize the following features of hypernuclei obtained in the fragmentation processes and new directions of the research:

1) Fragmentation reactions leading to the formation of hypernuclei can provide new insights into mechanisms of such processes, including the phase transition phenomena, and give access to the EoS of hypernuclear matter.

2) New hypernuclei can help to investigate the structure of nuclei by extending the nuclear chart into the strangeness sector [8–11,15]. Complex multi-hypernuclear systems incorporating more than two hyperons can be created in such energetic nucleus-nucleus collisions, *e.g.*, STAR at RHIC, CBM and NUSTAR experiments at FAIR, ALICE at LHC. Indeed, heavy-ion reactions may be the only conceivable method to go even beyond $|s| = 2$.

3) Important astrophysical states such as isospin asymmetric hypermatter produced at high nuclear densities and low temperatures in the core of neutron stars [12] can be addressed by studying hypernuclei, especially multi-hyperon ones, and those with extreme isospin.

4) Indications for new bound strange systems with extreme isospin have been found very recently: As discussed, the HypHI Collaboration has seen signals compatible with a neutral Λnn state [21], the FINUDA Collaboration claimed the observation of ${}^{6}_{\Lambda}$H events [41]. These exotic hypersystems may lead to the breakthrough in hyperphysics and they are now under intensive experimental [42] and theoretical [43, 44] investigation. The experimental confirmation of these states and search for new states at high-energy reactions has the highest priority [45, 46].

2 Production mechanisms for hypernuclei and the models

The formation processes of hypernuclei are quite different in central and peripheral ion collisions. There are indications that in central collisions of very high energy the coalescence mechanism, which assembles light hyperfragments from the produced hyperons and nucleons (including antibaryons), is essential [27, 28, 47–49]. Thermal models suggest also that only the lightest clusters, with mass numbers $A \lesssim 4$, can be noticeably produced in this way because of the very high temperature of the fireball ($T \approx 160\,\mathrm{MeV}$) [50,51]. On the other hand, it was noticed, some time ago, that the absorption of hyperons in spectator regions after peripheral nuclear collisions is a promising way for producing hypernuclei [52–55]. An important feature of peripheral collisions is that large pieces of nuclear matter around normal nuclear density at low temperature can be created as compared to highly excited nuclear matter at mid-rapidity. In the simplified picture, nucleons from overlapping parts of the projectile and target (participant zone) interact strongly with themselves and with other hadrons produced in primary and secondary collisions. Nucleons from non-overlapping parts do not interact intensively, and they form residual nuclear systems, which we call spectator residues or spectators. It is well established that moderately excited spectator residues ($T \lesssim 5$–$6\,\mathrm{MeV}$) are produced in such reactions [34–36,56]. The production of hyperons is associated with nucleon-nucleon collisions, *e.g.*, $\mathrm{p} + \mathrm{n} \to \mathrm{n} + \Lambda + \mathrm{K}^+$, or collisions of secondary mesons with nucleons, *e.g.*, $\pi^+ + \mathrm{n} \to \Lambda + \mathrm{K}^+$. Strange particles may be produced in the participant zone, however, particles can rescatter and undergo secondary

interactions. As a result the produced hyperons populate the whole momentum space around the colliding nuclei, including the vicinity of nuclear spectators, and can be captured by the spectator residues. A hyperon absorption in these residues should not change the whole reaction picture since the hyperon-nucleon forces are analogous to the nucleon-nucleon ones. General regularities of the decay of such hyper-residues into hyperfragments could be investigated with statistical models (*e.g.*, generalized Statistical Multifragmentation Model SMM [38–40]), which were previously applied for description of normal fragment production with great success [34–37].

At present the theoretical predictions of strangeness and hyperon production in hadron and ion reactions can be performed with various dynamical models employing similar general assumptions on the hadron transport in nuclei but with different methods of solution of the kinetic equations. In addition, the models have rather different features concerning hadron-hadron interactions and production of new particles. Involving various transport models is very important since we obtain knowledge about uncertainties in such calculations. At relatively low-energy elementary hadron collisions (less than 1–2 GeV in the center-of-mass system of colliding particles) the models use usually quite reliable approximations for the reaction channels supported by analysis of large amount of available experimental data. However, at higher energies, where hyperon formation is more essential, theoretical estimations are mostly used. For example, the Dubna Cascade Model (DCM) [55, 57, 58] involves the quark gluon string model (QGSM). The Ultrarelativistic Quantum Molecular Dynamics (UrQMD) model [59, 60] has adopted the string formation and its fragmentation according to the PYTHIA model for hard collisions. The Lund FRITIOF string model (including PYTHIA) is used in the Hadron String Model (HSD) [61], however, for simulations including in-medium self-energies of particles. The Giessen Boltzmann Uehling Uhlenbeck (GiBUU) model [54] has also implemented PYTHIA for reaction processes with the test particles representing the Wigner transform of the hadron Green's functions. All these models were used successfully for description of strangeness production [55, 62, 63]. The capture of produced Λ hyperons by nuclear species can be easily obtained within the potential [55] or coalescence [51] criteria. Recently we have developed a generalization of the coalescence model [64, 65], the coalescence of baryons (CB), which can be applied after the dynamical stage described, for example, by DCM, UrQMD, and HSD models. In such a way it is possible to form fragments of all sizes, from the lightest nuclei to the heavy residues, including hypernuclei within the same mechanism. The advantage of this procedure is the possibility to predict the correlations of yields of hypernuclei, including their sizes, with the rapidity on the event-by-event basis, that is very important for the planning of future experiments.

There is a connection between dynamical and statistical approaches: The DCM and GiBUU can directly calculate the parameters of residual nuclei obtained in peripheral relativistic ion collisions. In the case of simulations with UrQMD and HSD codes, besides the coalescence of baryons, one can "mark" non-interacting nucleons of the colliding nuclei and consider them as the ones forming the residues together with other captured baryons. In the following one can apply the statistical models for description of the final reaction stage (de-excitation of the residues [23, 54]) by taking into account, for example, the experimentally found relation between excitation energies and masses of the residues [37]. The disintegration of heavy hypersystems can be described by the generalized SMM [15, 38]. The statistical Fermi break-up model (FBM) is very the effective for the description of decay of light systems, and it was generalized to describe the disintegration of the hyper-residues [66]. In this way we have constructed a hybrid approach which can be directly used for the analysis of experimental data, as well as for evaluation of new experiments [23, 30, 31, 57, 67]. In particular, the models predict the formation of multi-hyperon systems [55], exotic hypernuclei and those beyond the driplines, which are hardly possible to obtain in other reactions [15, 23, 57].

3 Main regularities of hypernuclei formation

It was previously demonstrated [15, 23, 55, 57, 65] that the most effective way to find novel hypernuclei is to use the fragmentation of the projectile and target spectator residues, and detect particles from the target (or projectile) kinematic region. During the last several years this was under intensive analysis with various dynamical approaches (DCM, UrQMD, HSD). These studies have led to similar results [57, 65]. For example, in fig. 1 we show predictions of the yields of hyper-residues in collisions of relativistic ions in the wide range of projectile energies. The calculations were done with the DCM by taking into account all impact parameters as in experiment. Within this approach the absorption of Λ hyperons by spectators was described in ref. [55]: It takes place if the hyperon kinetic energy in the rest frame of the residual spectator is lower than the attractive potential energy generated by neighbouring nucleons, *i.e.*, the hyperon potential, which is around 30 MeV in matter at normal nuclear density ρ_0. This potential is calculated by taking into account the local density of the spectator residues, which can be less than ρ_0. In the dynamical simulations we follow the propagation of all particles including Λ-hyperons during the whole reaction time, up to about 100 fm/c, and take into consideration secondary rescattering/interaction processes, which may lead to the hyperon production, the hyperon absorption, and making the absorbed hyperons free. The predicted cross-sections for such strange spectator residues are about $\sim$ 1–100 mb (depending on the colliding nuclei), that is more than sufficient for modern detectors which can reliably measure cross-sections of about $\sim 1\,\mu$b. One observes a rapid increase of the yields with the incident beam energy around the threshold of Λ production and the saturation trend at the laboratory energy of about 5–10 A GeV and higher. Therefore, there are excellent opportunities to study projectile- and target-like

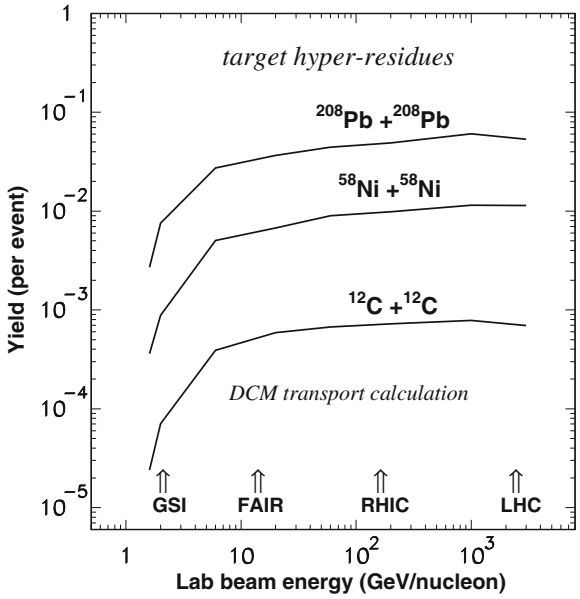

Fig. 1. Predicted yields of hyper-residues of targets in collisions of ^{12}C, ^{58}Ni, and ^{208}Pb beams with the same targets, as a function of the incident energy. Projectile energies corresponding to GSI, FAIR, RHIC, and LHC accelerators for the fixed targets are marked by arrows. The DCM calculations are integrated over all impact parameters, and normalized to one inelastic collision event (from ref. [57]).

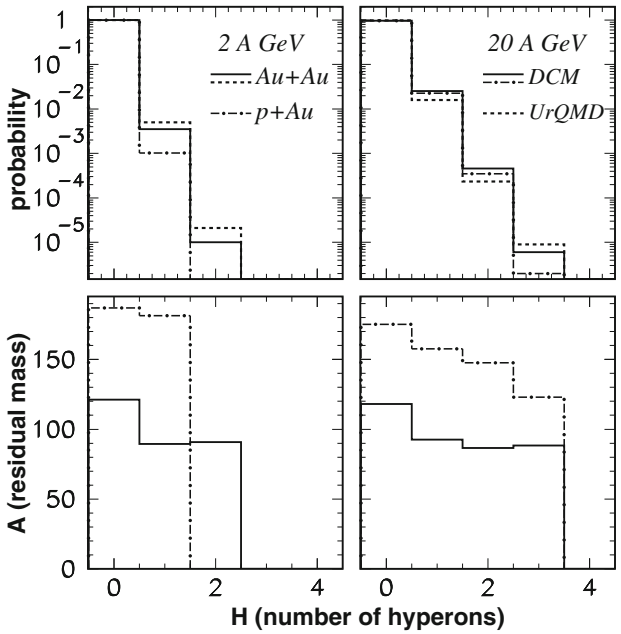

Fig. 2. Probability for formation of conventional and strange spectator residues (top panels), and their mean mass numbers (bottom panels) *vs.* the number of captured Λ hyperons (H), calculated with DCM and UrQMD model for p + Au and Au + Au collisions with energy of 2 GeV per nucleon (left panels), and 20 GeV per nucleon (right panels). The reactions and energies in the laboratory system are noted in the figure by different histograms (from ref. [55]).

hypernuclei at the FAIR facility, as well as at more powerful accelerators —RHIC and LHC. Because of this saturation, nearly the same results for single hypernuclei are obtained for all high energies (up to the TeV region). For this reason, in the following figures we show the GeV energies. However, the high-energy accelerators may have advantages, since the production of multi-strange hypersystems is more probable.

The characteristics of these hyper-residues are shown in more detail in fig. 2, in the case of heavy-ion collisions. The probability for the absorption of several hyperons falls with the hyperon number, however, it remains quite large, especially, at high projectile energy. One can see that even 3 Λ hyperons can be captured with significant probability ($\sim 10^{-5}$) and the capture of even more hyperons is feasible. It is important that both DCM and UrQMD lead to very close predictions. This opens an unique way for studying multi-strange systems with $|s| > 2$. It is instructive for experiments at very high energies, since the strangeness formation increases considerably. One can see by comparing the left and right top panels that the probability of the hyperon capture is less decreasing with H for the higher energy. Therefore, the high energetic reactions enhance the production of multi-hyperon nuclei. Masses of the hyper-residues are large, therefore, one can discuss formation of excited hypermatter at density around normal nuclear ones ρ_0. The subsequent disintegration of this hypermatter into normal and hyperfragments can proceed via fission and evaporation processes known well at low excitation energies. At high excitations this disintegration can give information about the liquid-gas-type phase transition and the equation of state of the hypermatter, similar to that obtained for the case of the normal nuclear matter [34, 56]. In addition, the products of such a disintegration can be exotic species, which cannot be obtained in other reactions.

The latter is illustrated in fig. 3, where we predict the yields of normal as well as hyperfragments after disintegration of a heavy system by assuming two absorbed hyperons, and the isotope composition which can be produced with special beams and targets [68, 69]. The calculations for this reaction stage were performed within the mentioned statistical approach (SMM), see refs. [15, 38] for more detail. The model assumes that a hot nuclear spectator with total mass (baryon) number A_0, charge Z_0, number of Λ hyperons H_0, and temperature T expands to a low-density freeze-out volume, where the system is in chemical equilibrium. The statistical ensemble includes all break-up channels composed of nucleons and excited fragments with mass number A, charge Z, and H is their number of Λ's. The primary fragments are formed in the freeze-out volume V. We use the excluded volume approximation $V = V_0 + V_f$, where $V_0 = A_0/\rho_0$, and parametrize the free volume $V_f = \kappa V_0$, with $\kappa \approx 2$. This and other parameters in the model are taken as in the case of statistical fragmentation and multifragmentation of normal nuclei, which give a very good description of the data (see, *e.g.*, [34–37]).

Nuclear clusters in the freeze-out volume are described as follows: light fragments with mass number $A < 4$

are treated as elementary particles with corresponding spin and translational degrees of freedom ("nuclear gas"). Their binding energies were taken from experimental data [8, 11, 34]. Fragments with $A = 4$ are also treated as gas particles with table masses, however, some excitation energy is allowed $E_x = AT^2/\varepsilon_0$ ($\varepsilon_0 \approx 16\,\mathrm{MeV}$ is the inverse volume level density parameter [34]), that reflects the presence of excited states in ^{4}He, $^4_\Lambda$H, and $^4_\Lambda$He nuclei. Fragments with $A > 4$ are treated as heated liquid drops. In this way one can study the nuclear liquid-gas coexistence of hypermatter in the freeze-out volume. The internal free energies of these fragments are parametrized as the sum of the bulk (F^B_A), the surface (F^S_A), the symmetry (F^{sym}_{AZH}), the Coulomb (F^C_{AZ}), and the hyperenergy (F^{hyp}_{AH}):

$$F_{AZH}(T,V) = F^B_A + F^S_A + F^{\mathrm{sym}}_{AZH} + F^C_{AZ} + F^{\mathrm{hyp}}_{AH}. \quad (1)$$

The first three terms are written in the standard liquid-drop form [38]:

$$F^B_A(T) = \left(-w_0 - \frac{T^2}{\varepsilon_0}\right) A,$$
$$F^S_A(T) = \beta_0 \left(\frac{T_c^2 - T^2}{T_c^2 + T^2}\right)^{5/4} A^{2/3},$$
$$F^{\mathrm{sym}}_{AZH} = \gamma \frac{(A - H - 2Z)^2}{A - H}. \quad (2)$$

The model parameters $w_0 = 16\,\mathrm{MeV}$, $\beta_0 = 18\,\mathrm{MeV}$, $T_c = 18\,\mathrm{MeV}$ and $\gamma = 25\,\mathrm{MeV}$ were extracted from nuclear phenomenology. The Coulomb interaction of the fragments is described within the Wigner-Seitz approximation, and F^C_{AZ} is taken as in ref. [34].

The new term is the free hyperenergy F^{hyp}_{AH}. We assume that it does not change with temperature, *i.e.*, it is determined solely by the binding energy of the hyperfragments. We have suggested the liquid-drop hyper term [38]:

$$F^{\mathrm{hyp}}_{AH} = (H/A) \cdot (-10.68A + 21.27A^{2/3}). \quad (3)$$

In this formula the binding energy is proportional to the fraction of hyperons in the system (H/A). The second part represents the volume contribution reduced by the surface term and thus resembles a liquid-drop parametrization based on the saturation of the nuclear interaction. As demonstrated in ref. [15] the formula gives a reasonable description of binding energies of known hypernuclei. A captured Λ hyperon can occupy the s-state deep inside nuclei, since it is not forbidden by the Pauli principle. For this reason adding this hyperon to nuclei is a more effective way to increase their binding energies than adding nucleons, especially for large species.

The break-up channels are generated according to their statistical weight. In the Grand Canonics this leads to the following average yields of individual fragments:

$$Y_{\mathrm{AZH}} = g_{\mathrm{AZH}} \cdot V_f \frac{A^{3/2}}{\lambda_T^3} \exp\left[-\frac{1}{T}\left(F_{AZH}(T,V) - \mu_{AZH}\right)\right],$$
$$\mu_{AZH} = A\mu + Z\nu + H\xi. \quad (4)$$

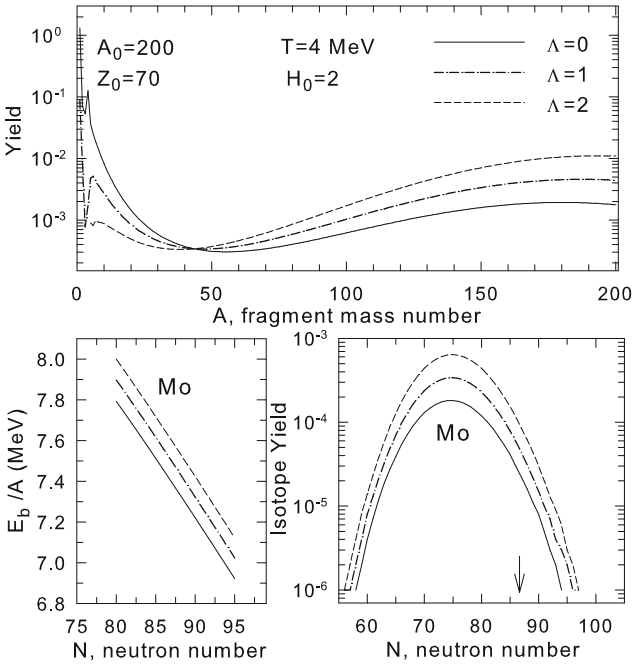

Fig. 3. Characteristics of normal fragments (solid lines) and hyperfragments with one (dashed lines) and two (dash-dotted lines) Λ hyperons produced after disintegration of an excited hypernuclear system with mass number $A_0 = 200$, charge $Z_0 = 70$, temperature $T = 4\,\mathrm{MeV}$, and containing two Λ hyperons ($H_0 = 2$). Top panel: Relative yields of fragments *vs.* their mass number. Bottom right panel: Relative isotope yields for molybdenum fragments ($Z = 42$) *vs.* the neutron number. The arrow indicates the neutron drip-line. Bottom left panel: Binding energies per baryon (E_b/A) of molybdenum hypernuclei for the neutron numbers around the neutron drip-line (from ref. [15].)

Here g_{AZH} is the ground-state degeneracy factor of species (A, Z, H), $\lambda_T = (2\pi\hbar^2/m_N T)^{1/2}$ is the nucleon thermal wavelength, m_N is the average nucleon mass. The chemical potentials μ, ν, and ξ are responsible for the mass (baryon) number, charge, and strangeness conservation in the system.

As a result, there is a wide distribution of produced fragments (top panel of fig. 3), similar to the one in the break-up of normal nuclei corresponding to the onset of the phase transition in finite systems. However, the hyperons are mainly concentrated in big fragments, since the presence of Λ hyperons increases the nuclear binding energy significantly, as one can see from the bottom-left panel demonstrating the binding energy of hypernuclei *vs.* the neutron number. It is clear from formula (3) that this increase is larger for bigger fragments. Here we should note that the shown decrease of the binding energy at large numbers of neutrons is obtained under the standard assumption on the nuclear symmetry energy coefficient γ, and an essential decreasing of this coefficient for neutron-rich isotopes is disregarded [15, 70]. This question, actual for neutron star matter, could also be clarified in future hypernuclear studies by taking into account the "gluing" effect of hyperons inside nuclei. The isotope distribution

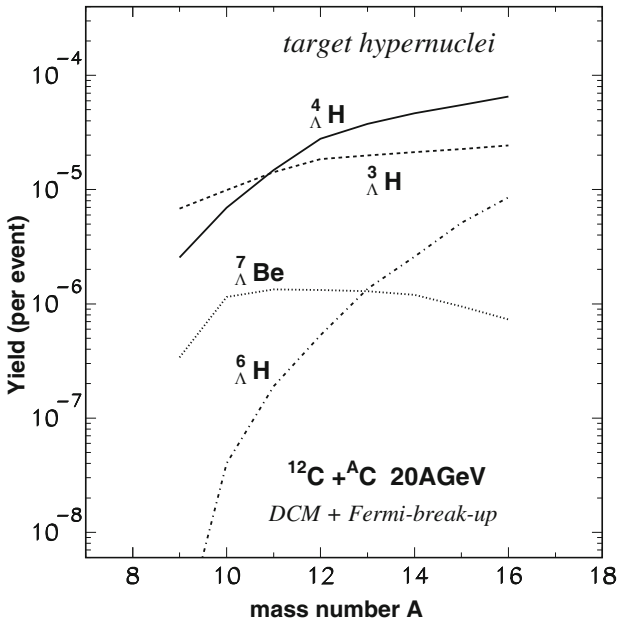

Fig. 4. Yields of light hypernuclei (see notations at the lines in the panel) obtained from target residues in collisions of projectile ^{12}C with target carbon isotopes *vs.* the isotope mass number A. The hybrid DCM and FBM calculations are integrated over all impact parameters, and normalized to one inelastic collision event. The projectile energy is 20 GeV per nucleon (from ref. [57]).

of produced nuclei (bottom-right panel) can go beyond the neutron drip-line for both normal nuclei and hypernuclei. Such normal nuclei are usually particle unstable, while the hypernuclei may be stable and may remain beyond the drip-line even after emission of few nucleons in the secondary de-excitation process. This is an original mechanism for producing exotic hypernuclei which are not feasible to obtain in other reactions.

Since the experimental methods for identification of light hypernuclei are most reliable we demonstrate in fig. 4 the new opportunity for producing exotic light hypernuclei by means of relativistic ion collisions using various targets. In this case the excited hyper spectator residues produced after the dynamical stage are mostly light systems. For their disintegration we have used the Fermi-break-up model generalized by including Λ hyperons in ref. [66]. In the microcanonical approximation we take into account all possible break-up channels, which satisfy the mass number, hyperon number (*i.e.*, strangeness), charge, energy and momentum conservations, and simulate the competition between these channels. The probability of each break-up channel *ch* is proportional to the occupied phase space and the statistical weight of the channel containing n particles with masses m_i $(i = 1, \ldots, n)$ can be calculated as

$$W_{ch}^{mic} \propto \frac{S}{G}\left(\frac{V_f}{(2\pi\hbar)^3}\right)^{n-1}\left(\frac{\prod_{i=1}^{n} m_i}{m_0}\right)^{3/2} \cdot\frac{(2\pi)^{\frac{3}{2}(n-1)}}{\Gamma(\frac{3}{2}(n-1))}\cdot\left(E_{kin}-U_{ch}^{C}\right)^{\frac{3}{2}n-\frac{5}{2}}, \quad (5)$$

where $m_0 = \sum_{i=1}^{n} m_i$ is the summed mass of the particles, $S = \prod_{i=1}^{n}(2s_i+1)$ is the spin degeneracy factor (s_i is the i-th particle spin), $G = \prod_{j=1}^{k} n_j!$ is the particle identity factor (n_j is the number of particles of kind j). E_{kin} is the kinetic energy of nuclei and U_{ch}^{C} is the Coulomb interaction energy between nuclei, which are related to the energy balance as described in ref. [66]. The table masses of both ground states and known excited states of (hyper)nuclei (see, *e.g.*, [8,11]) are included. Our calculations were performed on an event-by-event basis and can easily be filtered by the experimental conditions in order to take into account the experimental background for detection of hypernuclei [57]. As can be seen from fig. 4 by selecting the isotope composition of the projectile and target nucleus we can influence the composition of produced hypernuclei significantly. This is again a unique chance which can be realized in relativistic ion collisions. By comparing the yields one can learn about the details of the production mechanisms and the binding energy of hypernuclei. For example, the recent discovery of exotic $^{6}_{\Lambda}$H hypernuclei [41] is now discussed intensively [43,44], and the low statistics of traditional hypernuclear experiments is a serious problem. One can see that it is possible to increase the $^{6}_{\Lambda}$H relative yield nearly by two orders of magnitude by involving neutron-rich targets. The reason is that the probability of formation of neutron-rich (hyper)nuclei increases essentially as a results of the total increase of the neutron number in the system. This method can be applied for searching also for other exotic bound states. The experimental evidences for Λn and Λnn states in the projectile residue region were discussed recently [21, 22], and —if confirmed— the observed yields are consistent with the FBM production mechanism [23].

It is instructive to demonstrate a connection between formation of all fragments, *i.e.*, normal ones, large and small hypernuclei. This can be analyzed within the coalescence mechanism for producing fragments from the individual nucleons and hyperons obtained after the dynamical stage [65]. The criterion of the coalescence is the proximity of baryons in the velocity and coordinate space. A variation of the coalescence parameters within reasonable values does not change the general picture of the fragment formation. The selection of the adequate parameters can be directed by comparison with experiments. Below we show the results obtained with the parameters extracted from an analysis of the yield of normal fragments.

The total mass yields of the normal fragments and hyperfragments (with one bound Λ) are shown in fig. 5. The coalescence of baryons (the CB model) was applied after the UrQMD, for the reactions of relativistic energies initiated in ion collisions on carbon and gold targets. Though the yields are normalized per one inelastic event, one should take into account that only events with production of hyperons have been analysed in this case. For this reason there is no characteristic increase of the yield of normal fragments with masses around the projectile/target mass, which are caused by very peripheral collisions. One can see that the production of fragments of all sizes is possible. As expected, the yield of conventional fragments

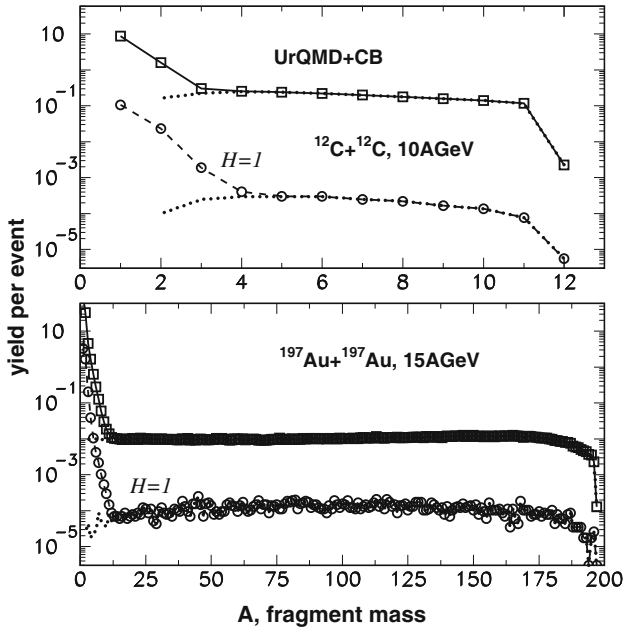

Fig. 5. Yields (per one inelastic event) of normal fragments (solid lines with squares) and hyperfragments with one captured Λ (notation $H = 1$, dashed lines with circles) *vs.* their mass number (A) in reactions induced by carbon and gold collisions. The dotted lines present the corresponding fragments originated from the spectator residues. The projectile lab energies are shown in panels. The calculations are performed within the hybrid UrQMD plus CB model, and integration over all impact parameters (see ref. [65]).

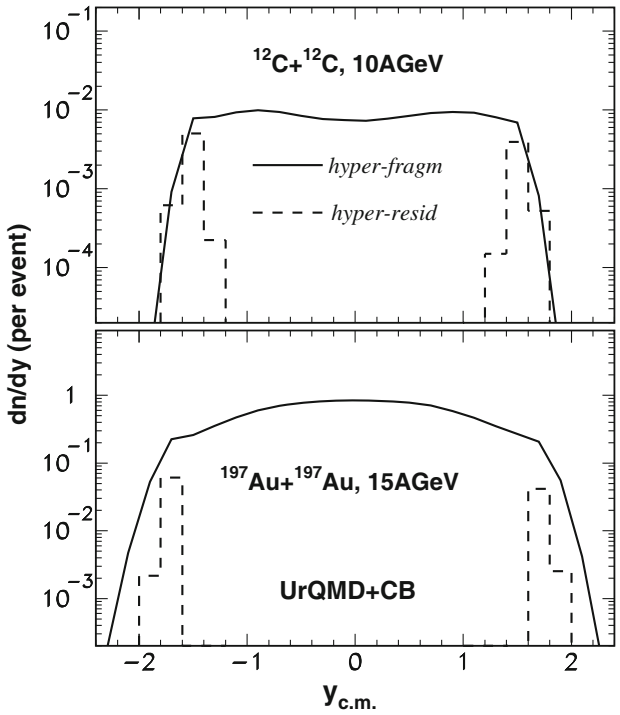

Fig. 6. Rapidity distributions (in the center-of-mass system, $y_{c.m.}$) of produced hyperfragments (solid lines) and hyper-residues (dashed lines) calculated within the UrQMD plus CB model (ref. [65]). The reactions, parameters and other notations are as in fig. 5.

is by few orders of magnitude higher than the yield of hyperfragments. Nevertheless, the production of hyperfragments is sufficient to be experimentally measured (see also [57]). It is a natural result of the coalescence that the yield of the lightest hyperfragments is dominating. However, the capture of hyperons by residues saturates the yield for large masses and leads to abundant production of heavy hyperfragments. Within this approach one can see clearly that nearly all normal fragments and hyperfragments with $A > 3$–4 in the carbon collisions, and with $A > 10$ in the gold collisions originate from the capture of Λ hyperons by spectator residues (dotted lines). As was mentioned we believe that these hyperfragments represent excited pieces of hypermatter whose evolution can be calculated with statistical models [15,38].

There is a relation between the formation mechanisms and the velocities of produced hyperfragments. Their total rapidity distributions are demonstrated in figs. 6 after UrQMD and CB calculations. One can see that the big fragments, which can come only from the residues, will be concentrated around the target and projectile rapidity (dashed lines). Whereas the small fragments, which are formed after the coalescence of fast baryons, can populate the midrapidity region also. It is interesting that in the carbon collisions the hyper-residues are responsible for producing nearly all hyperfragments in their kinematic regions. In the gold case, many new strange particles of relatively high energy are produced in this region, therefore, besides big hyperfragments coming from the residues additional energetic light hypernuclei can yield too. This correlation should be taken into account by planning the production of specific hypernuclei and analyzing the data: It is important that different reaction mechanisms, *e.g.*, the statistical disintegration of hyper-residues (a many-body process) and the coalescence of baryons in final states (a two-body process), may lead to different hypernuclei.

The lightest hypernuclei $^{3}_{\Lambda}$H and $^{4}_{\Lambda}$H are specially interesting: They can be easily identified by their decay into π^- and ^{3}He, and into π^- and ^{4}He, respectively. These correlations have been observed already in many heavy-ion experiments at high energies [19–21, 27, 28, 47, 48]. Such hypernuclei can serve as indicators for the production of hypermatter. In fig. 7 we show the rapidity distributions of these light hypernuclei in the same reactions. One can see an instructive behaviour: The $^{3}_{\Lambda}$H nuclei are essentially formed over all rapidities. As was mentioned, the central midrapidity region corresponds to a fireball with very high temperature contrary to the nearly cold remnants of the target and projectile. The larger nuclei ($^{4}_{\Lambda}$H) are more grouped at the target and projectile rapidities. This is the consequence of the reaction mechanism: The secondary interactions contributing considerably to the formation of hyperons with relatively low momenta, which can be captured by larger pieces of nuclear matter, happen mostly in the residue region. As was demonstrated in ref. [65] the saturation of the yields for single hypernuclei with energy concerns the light nuclei produced at the midrapidity

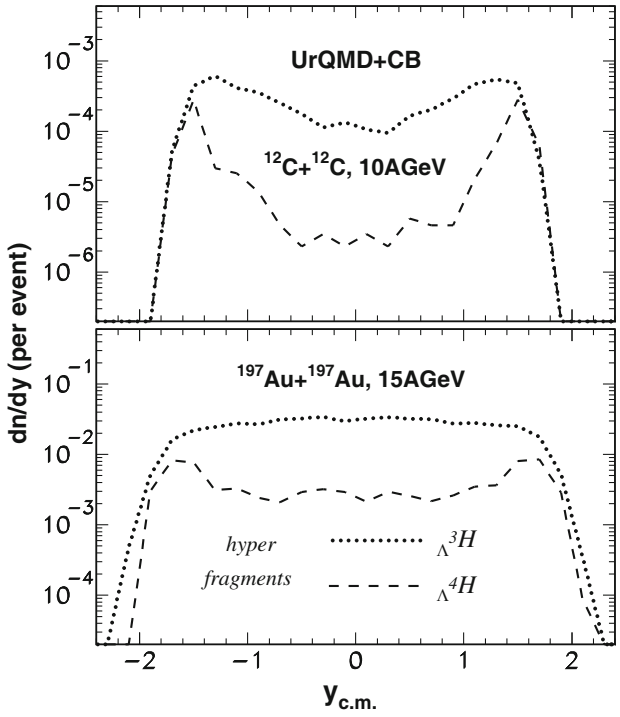

Fig. 7. Rapidity distributions of produced $^{3}_{\Lambda}$H (dotted lines) and $^{4}_{\Lambda}$H (dashed lines) hyperfragments in reactions as in fig. 6. The UrQMD and CB calculations are taken from ref. [65].

region too. It is because in the fireball region the primary hadron interactions lead to the production of high-energy hyperons, and, as a result, the nucleons and hyperons are far from each other in momentum space. Therefore, despite increasing the number of hyperons with the energy the total number of the coalescent hyperfragments does not increase considerably.

The correlation measurements (of pions, baryons and fragments) are the most promising tool for future research in this field. They allow for identification of hypermatter and can reveal the hypernuclei properties. For example, by detecting the momenta of their decay products one can find the life-time of the hypernuclei and their binding energies. By analyzing the decay of free Λ hyperons and hypernuclei in the same events one can investigate the unbound hyperon states in double hypernuclei. It is crucial for constraining the hyperon interaction in matter and determining the properties of hypermatter at low temperatures. As discussed, the last one is also important for compact astrophysical objects such as neutron stars [12]. The background of these correlation processes can be evaluated with the developed theory models too [57].

4 Conclusion

We conclude that relativistic collisions of hadron and ion with ions are a very promising source of hypermatter and hypernuclei. By comparing the previous results obtained with various models we note that it is a universal process and well established theoretically. A large amount of hypernuclei of all masses and in a wide range of isospin can be produced. Systematic investigations of multi-strange hypernuclei can be naturally performed in these reactions. The production of strangeness is possible at all rapidities, however, the most instructive results are expected in the target (or projectile) kinematic regions. This nicely corresponds to future BM@N and FAIR experiments. In this case the extraction of large pieces of nearly cold hypermatter becomes possible and its properties including the EoS can be investigated. In addition, new exotic hypernuclei can be formed in such reactions, and new methods of their investigation (*e.g.*, by using many-particle correlations) can be applied, which gives advantages over the traditional hypernuclear studies.

We also note that the general mechanism of such reactions leading to fragmentation and multifragmentation is well established for normal nuclear processes. Hyperons are also participating in such a process because the hyperon-nucleon interaction is of the same order as the nucleon-nucleon one. This universality leads to an important conclusion that any baryon with an attractive potential may be bound in a nucleus. It may concern the production of "charmed" and "bottom" nuclei after a possible capture of charmed (*e.g.*, Λ_c^+) and bottom (Λ_b^0) baryons. Nobody has observed such nuclei yet, real interaction potentials of such baryons are not known, therefore, this suggestion should be still considered as a hypothesis. In any case, a probability for production of these nuclei may be by several orders of magnitude lower than for conventional hypernuclei. However, very high energies and the presence of heavy residues in the target and projectile rapidity regions may provide an adequate place to search for the extension of nuclear physics into the new flavor dimensions. Obviously a first step for this experimental study would be a construction of a set up for reliable detection of rare decays associated with hypernuclei.

We thank our colleagues who have contributed to this research project: E. Bratkovskaya, N. Buyukcizmeci, K.K. Gudima, I.N. Mishustin, A. Sanchez Lorente, and H. Stöcker. This work was supported by the GSI Helmholtzzentrum für Schwerionenforschung and Hessian initiative for excellence (LOEWE) through the Helmholtz International Center for FAIR (HIC for FAIR), and by BMBF.

References

1. P.B. Demorest *et al.*, Nature **467**, 1081 (2010).
2. J. Antoniadis *et al.*, Science **340**, 1233232 (2013).
3. A. Gal, Phys. Rev. **152**, 975 (1966).
4. S. Nishizaki, Y. Yamamoto, T. Takatsuka, Prog. Theor. Phys. **105**, 607 (2001)
5. S. Nishizaki, Y. Yamamoto, T. Takatsuka, Prog. Theor. Phys. **108**, 703 (2002).
6. D. Lonardoni, S. Gandolfi, F. Pederiva, Phys. Rev. C **87**, 041303(R) (2013).
7. Y. Yamamoto, T. Furumoto, N. Yasutake, Th.A. Rijken, Phys. Rev. C **88**, 022801(R) (2013).

8. H. Bando, T. Mottle, J. Zofka, Int. J. Mod. Phys. A **5**, 4021 (1990).
9. J. Schaffner, C.B. Dover, A. Gal, C. Greiner, H. Stoecker, Phys. Rev. Lett. **71**, 1328 (1993).
10. W. Greiner, J. Mod. Phys. E **5**, 1 (1996).
11. O. Hashimoto, H. Tamura, Prog. Part. Nucl. Phys. **57**, 564 (2006).
12. J. Schaffner-Bielich, Nucl. Phys. A **804**, 309 (2008).
13. A. Gal, O. Hashimoto, J. Pochodzalla (Editors), Nucl. Phys. A **881**, 1 (2012) Special issue on *Progress in Strangeness Nuclear Physics*.
14. K. Morita *et al.*, Phys. Rev. C **91**, 024916 (2015).
15. N. Buyukcizmeci, A.S. Botvina, J. Pochodzalla, M. Bleicher, Phys. Rev. C **88**, 014611 (2013).
16. T. Hell, W. Weise, Phys. Rev. C **90**, 045801 (2014).
17. T.A. Armstrong *et al.*, Phys. Rev. C **47**, 1957 (1993).
18. H. Ohm *et al.*, Phys. Rev. C **55**, 3062 (1997).
19. HypHI Collaboration (T.R. Saito *et al.*), Nucl. Phys. A **881**, 218 (2012).
20. C. Rappold *et al.*, Nucl. Phys. A **913**, 170 (2013).
21. C. Rappold *et al.*, Phys. Rev. C **88**, 041001(R) (2013).
22. T.R. Saito (for the HypHI Collaboration), talks at the *ECT Workshop "Strange Hadronic Matter", Trento, Italy, 2011*, `http://www.ectstar.eu/` and *NUFRA2011 Conference, Kemer, Turkey, 2011*, `http://fias.uni-frankfurt.de/historical/nufra2011`.
23. A.S. Botvina, I.N. Mishustin, J. Pochodzalla, Phys. Rev. C **86**, 011601(R) (2012).
24. H. Takahashi *et al.*, Phys. Rev. Lett. **87**, 212502 (2001).
25. A. Sanchez Lorente, J. Pochodzalla, A. Botvina, Int. J. Mod. Phys. E **19**, 2644 (2010).
26. J. Pochodzalla *et al.*, Phys. Rev. C **35**, 1695 (1987).
27. The STAR Collaboration, Science **328**, 58 (2010).
28. ALICE Collaboration (B. Dönigus *et al.*), Nucl. Phys. A **904**, 547c (2013).
29. The PANDA Collaboration, `http://www-panda.gsi.de` and arXiv:physics/0701090.
30. `https://indico.gsi.de/event/superfrs3` (access to pdf files via timetable and key "walldorf").
31. C. Rappold, T.R. Saito, C. Scheidenberger, *Simulation Study of the Production of Exotic Hypernuclei at the Super-FRS (at GSI Scientific report 2012)*, GSI Report 2013-1 (2013) `http://repository.gsi.de/record/52079`.
32. *NICA White Paper*, `http://theor.jinr.ru/twiki-cgi/view/NICA/WebHome`, `http://nica.jinr.ru/files/BM@N`.
33. M. Danysz, J. Pniewski, Philos. Mag. **44**, 348 (1953).
34. J.P. Bondorf, A.S. Botvina, A.S. Iljinov, I.N. Mishustin, K. Sneppen, Phys. Rep. **257**, 133 (1995).
35. H. Xi *et al.*, Z. Phys. A **359**, 397 (1997).
36. R.P. Scharenberg *et al.*, Phys. Rev. C **64**, 054602 (2001).
37. R. Ogul *et al.*, Phys. Rev. C **83**, 024608 (2011).
38. A.S. Botvina, J. Pochodzalla, Phys. Rev. C **76**, 024909 (2007).
39. S. Das Gupta, Nucl. Phys. A **822**, 41 (2009).
40. V. Topor Pop, S. Das Gupta, Phys. Rev. C **81**, 054911 (2010).
41. M. Agnello *et al.*, Nucl. Phys. A **881**, 269 (2012).
42. J-PARC E10 Collaboration, Phys. Lett. B **729**, 39 (2014).
43. E. Hiyama, S. Ohnishi, M. Kamimura, Y. Yamamoto, Nucl. Phys. A **908**, 29 (2013).
44. A. Gal, D.J. Millener, Phys. Lett. B **725**, 445 (2013).
45. *XI International Conference on Hypernuclear and Strange Particle Physics, Barcelona, Spain, 2012*, `http://icc.ub.edu/congress/HYP2012/talks.php`.
46. *NUFRA2013: 4-th International Conference on Nuclear Fragmentation, Kemer, Turkey, 2013*, `http://fias.uni-frankfurt.de/historical/nufra2013`.
47. Y.-G. Ma (for the STAR/RHIC Collaboration), talk at the *NUFRA2013 Conference, Kemer, Turkey, 2013*, `http://fias.uni-frankfurt.de/historical/nufra2013`.
48. L. Xue *et al.*, Phys. Rev. C **85**, 064912 (2012).
49. P. Camerini (for the ALICE/LHC Collaboration), talk at the *NUFRA2013 Conference, Kemer, Turkey, 2013*, `http://fias.uni-frankfurt.de/historical/nufra2013`.
50. A. Andronic, P. Braun-Munzinger, J. Stachel, H. Stöcker, Phys. Lett. B **697**, 203 (2011).
51. J. Steinheimer, K. Gudima, A. Botvina, I. Mishustin, M. Bleicher, H. Stöcker, Phys. Lett. B **714**, 85 (2012).
52. M. Wakai, H. Bando, M. Sano, Phys. Rev. C **38**, 748 (1988).
53. Z. Rudy, W. Cassing *et al.*, Z. Phys. A **351**, 217 (1995).
54. Th. Gaitanos, H. Lenske, U. Mosel, Phys. Lett. B **675**, 297 (2009).
55. A.S. Botvina, K.K. Gudima, J. Steinheimer, M. Bleicher, I.N. Mishustin, Phys. Rev. C **84**, 064904 (2011).
56. J. Pochodzalla, Prog. Part. Nucl. Phys. **39**, 443 (1997).
57. A.S. Botvina, K.K. Gudima, J. Pochodzalla, Phys. Rev. C **88**, 054605 (2013).
58. V.D. Toneev, N.S. Amelin, K.K. Gudima, S.Yu. Sivoklokov, Nucl. Phys. A **519**, 463c (1990).
59. S.A. Bass *et al.*, Prog. Part. Nucl. Phys. **41**, 225 (1998).
60. M. Bleicher *et al.*, J. Phys. G **25**, 1859 (1999).
61. W. Cassing, E.L. Bratkovskaya, Phys. Rev. C **78**, 034919 (2008).
62. E.L. Bratkovskaya *et al.*, Phys. Rev. C **69**, 054907 (2004).
63. C. Hartnack *et al.*, Phys. Rep. **510**, 119 (2012).
64. W. Neubert, A.S. Botvina, Eur. Phys. J. A **7**, 101 (2000).
65. A.S. Botvina *et al.*, Phys. Lett. B **742**, 7 (2015).
66. A.S. Lorente, A.S. Botvina, J. Pochodzalla, Phys. Lett. B **697**, 222 (2011).
67. A.S. Botvina *et al.*, Nucl. Phys. A **881**, 228 (2012).
68. Th. Aumann, Progr. Part. Nucl. Phys. **59**, 3 (2007).
69. H. Geissel *et al.*, Nucl. Instrum. Methods Phys. Res. B **204**, 71 (2003).
70. H. Imal *et al.*, Phys. Rev. C **91**, 034605 (2015).